

# Excitons in QED<sub>3</sub> and spin response in a phase-fluctuating *d*-wave superconductor

Babak H. Seradjeh<sup>1,\*</sup> and Igor F. Herbut<sup>2</sup>

<sup>1</sup>*Department of Physics and Astronomy, University of British Columbia, Vancouver, BC, Canada V6T 1Z1*

<sup>2</sup>*Department of Physics, Simon Fraser University, Burnaby, BC, Canada V5A 1S6*

We study the particle-hole exciton mode in the QED<sub>3</sub> theory of a phase-fluctuating *d*-wave superconductor in ladder approximation. We derive a Schrödinger-like equation for the exciton bound state and determine the conditions for its existence. We find the dispersion of this mode below the particle-hole continuum and compare our results with the resonance observed in neutron scattering measurements in cuprates.

## I. INTRODUCTION

Strong electronic correlations in high-temperature superconductors are believed to underlie their rich phenomenology. The superconducting gap in these materials exhibits *d*-wave symmetry with four nodes. Since the gap vanishes and changes sign at these nodes, the low-energy fermionic excitations have linear, Dirac-like, dispersion. An important probe of the correlations of these nodal quasiparticles is provided by inelastic neutron scattering measurements, which give us information about the momentum and energy dependence of the correlations of electronic spin degrees of freedom through their coupling to scattering neutrons. Over the past decade a consistent experimental picture of these correlations has been emerging in different families of cuprates, so far the exclusive hosts of high-temperature superconductivity. These include the double-layer [1–5] Bi- and Y- and the single-layer [6–11] La- and Tl-based families. The salient features of this picture are the following: (1) A resonance peak at the antiferromagnetic ordering wave vector,  $(\pi, \pi)$ , at a resonance energy  $\omega_{\text{res}}$  ( $\approx 41$  meV in optimally doped YBCO); (2) A two-dimensional [12] incommensurate structure *below* the resonance energy with maxima located at  $(\pi \pm \delta, \pi)$  and with a possible weak inward dispersion toward  $(\pi, \pi)$  as  $\omega \rightarrow \omega_{\text{res}}$ ; (3) An incommensurate structure *above* the resonance with outward dispersion away from  $(\pi, \pi)$  for higher energies. The above dispersions have been taken to suggest that the commensurate and incommensurate peaks may have a common origin.

In addition, the response is usually not discernible from the background below a certain energy, referred to as the “spin gap.” However, for the sake of clarity, we reserve the label “spin gap” strictly for the minimum value of particle-hole continuum,  $\omega_{\text{sg}}$ , and call the former “spin response threshold.” Thus, whether the observed signals at  $(\pi, \pi)$  and  $\omega_{\text{res}}$ , and/or incommensurate peaks are true resonances is closely linked to the question of whether they occur below the corresponding spin gap. Accordingly, one could think of two possible theoretical scenarios.

In the first scenario, there is no true resonance in the system, that is, no particle-hole bound state, and the peaks are merely the maxima of the spin response. The nodal quasiparticles will have a finite spin gap everywhere except at the nodes. At  $(\pi, \pi)$ , the peak would be interpreted as the overlap of the four incommensurate responses, one for each node, at the center. The spin gap and the spin response threshold are the same in this scenario. Usually this should also mean that the central peak falls off slowly as  $1/\omega$ , rather than being sharp. However, as noted above, the central peak observed in experiment seems to be very sharp, in some cases limited only by the energy resolution of the measurement.

In the second scenario, there would be a true resonance below the spin gap given by a  $\delta$ -function in the spin response, due to the formation of particle-hole bound states—the so-called spin excitons. In this scenario, the spin gap is distinct from the spin response threshold. It would still be important to determine the continuum response so we could decide what effects derive from which source. However, it would also be very important to determine the existence (or lack of) and the properties of such excitons in a candidate theory of cuprates.

In this paper, we study the existence of spin excitons within the QED<sub>3</sub> effective theory of underdoped cuprates [13–16]. The QED<sub>3</sub> theory describes a *d*-wave superconductor in which the phase of the superconducting order parameter is fluctuating. These phase fluctuations are encoded in a pair of  $U(1)$  gauge fields, the Berry gauge field and the Doppler gauge field, that couple to quasiparticle’s spin and charge degrees of freedom, respectively. Both gauge fields are massive in the superconducting phase, which, accordingly, exhibits sharp nodal excitations. As the system is underdoped, however, the phase-fluctuations grow stronger and eventually destroy the phase coherence of the superconducting order parameter. The resulting state may be shown to be insulating [17]. Whereas outside the superconductor the Doppler gauge field remains massive, the Berry gauge field becomes massless. This allows the general chiral symmetry breaking instability in the QED<sub>3</sub> [18, 19] to become operative, which in the present context implies the antiferromagnetic ordering in the system [14, 20].

Herbut and Lee [21] have previously calculated the QED<sub>3</sub> spin response in the superconducting phase in a low-energy approximation and found no exciton res-

---

\*Electronic address: babak@physics.ubc.ca

onance. In their approach the Berry gauge-field propagator in the superconducting phase was approximated by a constant, equal to its infrared mass. This result falls therefore into the first scenario discussed above. In the present paper we go beyond this “constant mass” approximation by including the momentum-dependence of the inverse propagator of the Berry gauge field, which becomes linear at high momenta. We do so by considering the scalar vertex for the spin response in a ladder approximation and by reducing the problem to an approximate Schrödinger equation that describes the formation of particle-hole bound states in the  $d$ -wave superconductor. We find that, for a strong enough coupling between the nodal quasiparticles mediated by the Berry gauge field such bound states exist. We derive their dispersion and compare our results with the experimental picture outlined above. However, due to the inherent gauge dependence of our ladder approximation we cannot definitely determine whether, for the physical values of parameters, QED<sub>3</sub> theory of cuprates is in this strong-coupling regime.

We note that the resonance is absent in La-cuprates. This could be due to different physics from competing stripe order that is known to exist in this family and results in a smaller critical temperature,  $T_c$ . Alternatively, within our theory, one might expect the resonance to be harder to discern from the incommensurate structure for a smaller  $T_c$ . See Sec. V for a discussion.

The paper is organized as follows: In Sec. II we formulate the ladder approximation for the scalar vertex and the spin response. In Sec. III we derive the Schrödinger equation for excitons, find the resulting expression for resonant spin response, and determine the conditions for their existence. In Sec. IV we discuss the dispersion of the excitons and compare with experiments. We summarize our results in Sec. V where we also comment on the issue of gauge dependence mentioned above. The details of some of our calculations are given in two appendices.

## II. LADDER APPROXIMATION

The spin part of the effective action for the nodal quasiparticles in the fluctuating  $d$ -wave superconductor [17] is given by

$$S = \int d^3r \sum_{i=1}^N \bar{\psi}_i \gamma_\mu (v_{i,\mu} \partial_\mu - i g a_\mu) \psi_i + \frac{1}{2} \int \frac{d^3p}{(2\pi)^3} a_\mu(-p) D_{\mu\nu}^{-1}(p) a_\nu(p), \quad (1)$$

where the number of flavours,  $N = 2$ , is the number of pairs of nodes. The bare value of the coupling  $g$  is unity. The Dirac spectrum is assumed for quasiparticles near the nodes with anisotropic velocities  $v_{1,\mu} = (1, v_F, v_\Delta)$  and  $v_{2,\mu} = (1, v_\Delta, v_F)$ . Here  $v_F/v_\Delta \sim 10$  is the ratio of the Fermi velocity to the gap gradient at the node. We will set  $v_F = v_\Delta$  throughout our calculations and restore

their values by rescaling the corresponding momenta at the end. Only the transverse components of the gauge field enter the action in Eq. (1): The gauge-field propagator has the form  $D_{\mu\nu}(p) = (\delta_{\mu\nu} - (1 - \xi)\hat{p}_\mu\hat{p}_\nu)D(p)$ , where [21]

$$D(p) = \frac{\pi}{4|p|} F\left(\frac{m}{|p|}\right), \quad (2)$$

$$F(z) = (4z^2 + 1) \tan^{-1} \frac{1}{2z} - 2z, \quad (3)$$

and  $\xi$  signifies a (nonlocal) gauge-fixing term [22]. The gauge field has a mass  $D^{-1}(0) = 12m/\pi$ . At high energies,  $D^{-1}(p) \sim |p|$ , which is an exact result [23]. Most of what we will say about excitons in QED<sub>3</sub> does not depend on the exact form of the interpolation between the infrared mass and the ultraviolet linear dependence of  $D^{-1}(p)$ , but for the sake of definiteness we will present our results for this particular form of the propagator, which is found from the dual theory of Refs. 24 and 17.

The spin operator,  $S_z$ , is related to the Dirac fields through [14],

$$\bar{\psi}_i(r) \psi_i(r) = 4 \cos(2\mathbf{K}_i \cdot \mathbf{r}) S_z(r),$$

where  $\mathbf{K}_{1,2} = (\pm k_F, k_F)$  denote the positions of two of the nodes in the Brillouin zone. We assume spin-rotational symmetry. Thus,  $\chi_{\mu\nu}(\mathbf{k}, \omega) = \langle S_\mu(-\mathbf{k}, -\omega) S_\nu(\mathbf{k}, \omega) \rangle = \delta_{\mu\nu} \chi(\mathbf{k}, \omega)$ , where  $\chi(\mathbf{k}, \omega) = \langle S_z(-\mathbf{k}, -\omega) S_z(\mathbf{k}, \omega) \rangle$ . Writing  $\mathbf{k} = 2\mathbf{K}_i + \mathbf{p}$ , we find

$$\chi(p) = \frac{1}{16} \int d^3r e^{-ip \cdot r} \sum_{ij} \langle \bar{\psi}_i(r) \psi_i(r) \bar{\psi}_j(0) \psi_j(0) \rangle. \quad (4)$$

In order to calculate the spin response in the QED<sub>3</sub> action we will adopt a ladder approximation for the four-point correlator  $\chi(p)$ , shown diagrammatically in FIG. 2. The first diagram represents the “bare” spin response in the absence of gauge field interactions. We denote it by  $\chi_0(p)$ .

It is standard to reformulate the ladder approximation in terms of gauge-field-induced corrections to the scalar vertex for the interaction between the external source (neutrons) and spinons. These vertex corrections are shown in FIG. 2. Defining the scalar vertex,  $\Gamma(k, p)$ , as the amputated diagram (without the external legs) on the left-hand side, we have

$$\chi(p) = -\frac{N}{16} \int \frac{d^3k}{(2\pi)^3} \text{tr} [G_0(k) \Gamma(k, p) G_0(k + p)], \quad (5)$$

where  $G_0(k) = -i\gamma_\mu k_\mu/k^2$  is the bare four-component spinon propagator in the superconducting state. From FIG. 2 we see that the scalar vertex satisfies the following Bethe-Salpeter equation,

$$\Gamma(k, p) = \mathbb{1} - g^2 \int \frac{d^3q}{(2\pi)^3} \gamma_\mu G_0(q) \Gamma(q, p) G_0(q + p) \times \gamma_\nu D_{\mu\nu}(k - q). \quad (6)$$

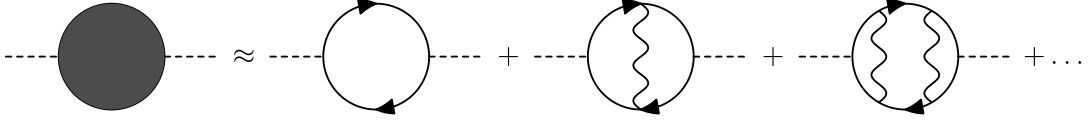
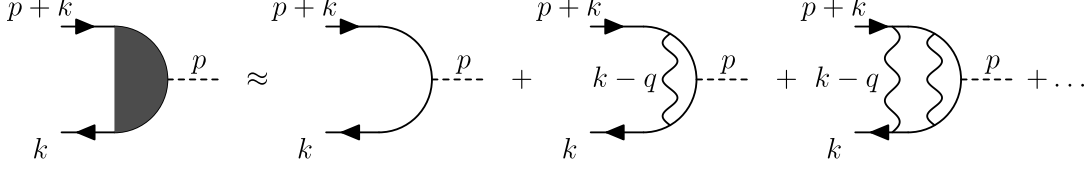


FIG. 1: Ladder approximation for the spin response

FIG. 2: Ladder approximation for the scalar vertex,  $\Gamma(k, p)$ .

We may use the symmetries of the QED<sub>3</sub> action to expand the scalar vertex in terms of form factors [25],

$$\Gamma(k, p) = \mathbb{1}F_1(k, p) + \sigma_{\mu\nu}k_\mu p_\nu F_2(k, p) + \gamma_\mu k_\mu F_3(k, p) + \gamma_\mu p_\mu F_4(k, p). \quad (7)$$

Here,  $\sigma_{\mu\nu} = \frac{1}{2}[\gamma_\mu, \gamma_\nu]$ . Then, Eq. (6) is reduced to

$$F_i(k, p) = \delta_{i1} + \int \frac{d^3q}{(2\pi)^3} \sum_{j=1}^4 K_{ij}(k, q, p) F_j(q, p), \quad (8)$$

with the matrix  $K_{ij}$  having a block-diagonal form in terms of two two-by-two matrices. For the reasons explained below the most important element is

$$K_{11}(k, q, p) = (2 + \xi)g^2 \frac{q \cdot (q + p)}{q^2(q + p)^2} D(k - q). \quad (9)$$

The block-diagonal form of  $K_{ij}$  implies that the form factors  $F_3$  and  $F_4$  completely decouple from  $F_1$  and  $F_2$ . Together with Eq. (6), which implies that  $F_3$  and  $F_4$  do not contribute to the function  $\chi$ , this allows us then to neglect them altogether for the purpose of calculating the spin response.

Within the ladder approximation for the scalar vertex, our manipulations have so far been exact. At this point, we notice that the dominant contribution to  $\chi$  comes from  $F_1$ , which is of order  $g^0$ . Since  $F_2 \sim g^2$ , we will then neglect  $F_2$  to obtain the set of equations [26, 27],

$$\chi(p) = \frac{N}{4} \int \frac{d^3k}{(2\pi)^3} \frac{k \cdot (k + p)}{k^2(k + p)^2} F_1(k, p), \quad (10)$$

$$F_1(k, p) = 1 + \lambda \int \frac{d^3q}{(2\pi)^3} \frac{q \cdot (q + p)}{q^2(q + p)^2} D(k - q) F_1(q, p), \quad (11)$$

for the spin response, with  $\lambda = (2 + \xi)g^2$  as the (gauge-dependent) coupling strength. These equations provide the basis for our further study of the exciton modes in QED<sub>3</sub>. For a constant  $D(k - q)$  they reproduce the results of Ref. 21.

Note that Eqs. (11) and (10) explicitly depend on the choice of gauge. This arises because the ladder diagrams in FIG. 2 are not gauge-invariant if the bare fermion propagator is used. The gauge invariance can be restored by choosing the (non-local) gauge-fixing parameter  $\xi$  so that the bare fermion propagator satisfies the usual Ward-Takahashi identity with the vertex. In principle this procedure will yield a momentum-dependent function,  $\xi(p)$  [27]. With  $m = 0$ , we find Nash's gauge  $\xi = 2/3$  [28] whereas in the opposite limit of constant-mass approximation one finds Feynman's gauge,  $\xi = 1$ . In the rest of the paper, we choose to work with a momentum-independent gauge-fixing parameter  $\xi$  for simplicity.

### III. EXCITONS IN QED<sub>3</sub>

Our strategy to solve the vertex function is to obtain a (set of) differential equation(s) from the integral equation (11). This is similar to the classic derivation of exciton bound states in metals and semiconductors [29, 30]. We will show that there is an approximate Schrödinger-like equation that captures the bound-state content of the vertex function. Similar Schrödinger equations have been derived before for the non-relativistic limit of vertex functions in QED [31, 32]. Based on this Schrödinger equation, we will determine the conditions for the existence of the exciton bound states.

#### A. Schrödinger equation

Let us define a generalized response

$$\Phi(r, p) = \sigma_\mu \sigma_\nu \int \frac{d^3k}{(2\pi)^3} \frac{k_\mu(k + p)_\nu}{k^2(k + p)^2} e^{ik \cdot r} F_1(k, p), \quad (12)$$

where  $\sigma_\mu = (\sigma_1, \sigma_2, \sigma_3)$  are Pauli matrices (up to cyclic permutations). Then Eqs. (10) and (11) may be written

as

$$\chi(p) = \frac{N}{4} \text{tr} [\Phi(0, p)] \equiv \frac{N}{4} \phi(0, p), \quad (13)$$

$$F_1(q, p) = 1 + \lambda \int d^3r e^{-iq \cdot r} D(r) \phi(r, p). \quad (14)$$

Note that  $r$  is a real-space variable and  $D(r)$  indicates the real-space gauge-field propagator.

We see that

$$-[(ip + p \times \sigma) \cdot \partial + \partial \cdot \partial] \Phi(r, p) = \delta^{(3)}(r) + \lambda D(r) \text{tr} [\Phi(r, p)]. \quad (15)$$

We may shift away the momentum  $p$  (which enters the equation only as a parameter) in the derivative by completing the square. This is achieved by a phase transformation of the form,

$$\Phi \rightarrow \Phi' = \exp \left[ \frac{1}{2} (ip + p \times \sigma) \cdot r \right] \Phi. \quad (16)$$

We note that  $\phi'(0, p) = \phi(0, p)$ . The transformed equation is, then,

$$[-\partial \cdot \partial + (p/2)^2] \Phi' - \lambda D(r) e^{\frac{1}{2} \sigma \cdot L} \text{tr} [e^{-\frac{1}{2} \sigma \cdot L} \Phi'] = \delta^{(3)}(r), \quad (17)$$

Where we have denoted the orbital angular momentum of the particle-hole system by  $L = r \times p$ . This is an exact mapping of the integral equation (11) to a set of coupled Schrödinger-like differential equations.

Even though we have succeeded in deriving a set of differential equations for our vertex function, they are still very complicated. However, for the purpose of studying the bound-state content of the vertex function, we may simplify these equations further down to a single Schrödinger-like equation. A numerical solution seems to be the only useful alternative. As shown in Appendix A, this approximate, decoupled equation is given by

$$[(p/2)^2 - \partial \cdot \partial - V_{\text{eff}}(r, p, m)] \phi'(r, p) = \delta^{(3)}(r), \quad (18)$$

where, for  $0 < |p| < 2m$ ,

$$V_{\text{eff}} = \lambda \left( 1 - \frac{\lambda \sin^2 \theta}{16} \right) \cosh^2 |L/2| D(r). \quad (19)$$

Here,  $\theta = \cos^{-1}(\hat{p} \cdot \hat{r})$ . We expect Eq. (18) to provide a valid description of the bound states for an adequately short-ranged interaction  $D(r)$ . This is the case when  $0 < |p| < 2m$ . For  $|p| > 2m$ , Eq. (19) is valid only at short distances. At large distances  $r \gg (|p| - 2m)^{-1}$ , the potential becomes infinite for  $\theta > \sin^{-1}(2m/|p|)$ :

$$V_{\text{eff}} \sim -\frac{\lambda^2}{p^2} \sinh^2 |L| D^2(r) \rightarrow -\infty. \quad (20)$$

We note that in the case of constant-mass approximation [21] for which  $D(r) \sim \delta^{(3)}(r)$ , and also for  $p = 0$  in the general case, Eq. (18) follows exactly from Eq. (17) with  $V_{\text{eff}}(r) = \lambda D(r)$ .

## B. Resonant spin response

We may now find  $\chi(p)$  by solving the following three-dimensional Schrödinger equation for the eigenvalue  $e_n(|p|, m)$  and the normalized eigenfunction  $\psi_n(r, |p|, m)$ ,

$$[-\partial \cdot \partial - V_{\text{eff}}] \psi_n = e_n \psi_n. \quad (21)$$

Then,

$$\chi(p) = \frac{N}{4} \phi'(0, p) = N \sum_n \frac{|\psi_n(0, |p|, m)|^2}{4e_n(|p|, m) + p^2}. \quad (22)$$

By analytically continuing to real frequencies,  $p_0 \rightarrow -i\omega + 0^+$ , and denoting  $p_M = \sqrt{\mathbf{p}^2 - \omega^2}$ , we find that since  $\Im e_n(p_M, m) = 0$  the imaginary part of the spin response observed in experiment is given by

$$\Im \chi(p_M) = N \sum_n \pm |\psi_n(0, p_M, m)|^2 \delta(p_M^2 + 4e_n(p_M, m)) \quad (23)$$

where the sign  $\pm = \text{sgn}(\omega) \text{sgn}(1 + \partial e_n(p_M, m)/\partial p_M^2)$ . If  $e_n(p_M, m)$  were not real there would be no  $\delta$ -function, hence no resonance.

From Eq. (23), we see that the necessary and sufficient condition for the existence of excitonic resonances at  $\mathbf{p}$  and  $\omega < |\mathbf{p}|$  is that our Schrödinger equation (21) admits bound state solutions with real and negative eigenvalues,  $e_b$ , that solve the equation

$$e_b(p_c, m) = -\frac{p_c^2}{4}. \quad (24)$$

We will now study the existence of such bound states.

## C. Existence of excitons

As shown in Appendix B the gauge-field propagator  $D(r)$  scales as  $1/r^2$ . For  $|p| > 0$ , we may rescale the space as  $|p|r \equiv z$  to see that the energy spectrum satisfies the scaling relation

$$e_b(|p|, m) = p^2 \varepsilon_b(2m/|p|). \quad (25)$$

The scaling function  $\varepsilon_b$  is the bound-state energy eigenvalue for the rescaled Schrödinger equation,

$$[-\nabla_z^2 - \tilde{V}_{\text{eff}}(z, \mu)] \psi_b(z, \mu) = \varepsilon_b(\mu) \psi_b(z, \mu), \quad (26)$$

where  $\mu = 2m/|p|$  and the rescaled potential is

$$\tilde{V}_{\text{eff}}(z, \mu) = \frac{1}{p^2} V_{\text{eff}} \left( \frac{z}{|p|}, 1, \frac{\mu|p|}{2} \right). \quad (27)$$

The potential  $\tilde{V}_{\text{eff}}$  has an inverse-square form for small  $z$ . The condition (24) for the resonant response is satisfied for  $\varepsilon_b(\mu_c) = -1/4$ ; then,  $p_c = 2m/\mu_c$ .

The inverse-square potential is an instance of conformal anomaly, i.e., the breakdown of scale symmetry in

quantum mechanics. The potential  $-\lambda/16z^2$  has an infinite number of negative energies for  $\lambda > \lambda_0^* = 4$  and is unbounded from below [33]. Thus, in this “strong-coupling” regime, the problem needs to be renormalized for it to be physically meaningful. Although there are different ways of doing so, the result is unique [34]. The inverse-square potential has a single renormalized bound-state. The energy of the renormalized bound-state cannot be determined within the theory; it is an input of the theory either from experiment, or from the physics at higher energies, beyond the domain of physical validity of the potential. The continuum spectrum that is renormalized into a single bound-state is called the “conformal tower.” The bound-state wave function is given by

$$\psi_0(z) = \sqrt{\frac{\kappa^3}{2\pi}} \frac{K_0(\kappa|z|)}{\sqrt{\kappa|z|}},$$

where  $-\kappa^2$  is the renormalized bound-state energy, and  $K_0$  is the modified Bessel function of the second kind.

For  $\mu \geq 1$  the potential  $\tilde{V}_{\text{eff}}$  decays exponentially at large distances. However, the inverse-square form at small  $z$  is expected to be sufficient for the existence of a conformal tower in the strong coupling  $\lambda > \lambda^*$ . By using  $\psi_0$  as a trial wave function to calculate the energy one can check that this expectation is met for  $\lambda^*/\lambda_0^* \approx 1.268$ . The corresponding critical charge is given by  $g_c \approx 2.252/\sqrt{2+\xi}$ . In Nash’s and Feynman’s gauge, for example, one finds  $g_{c,N} = 1.379$  and  $g_{c,F} = 1.300$ , respectively. The strong-coupling regime is found for  $g > g_c$ .

For  $0 \leq \mu < 1$ , the potential  $\tilde{V}_{\text{eff}} \sim -e^{2(\sin\theta - \mu)|z|} \rightarrow -\infty$  for  $\theta > \sin^{-1}\mu$ . So it is less clear whether the conformal tower would exist in this limit. However, the same way as above and by choosing  $\kappa > (1 - \mu)/2$ , we have checked that the conformal tower still persists for the same strong-coupling regime. This result reflects the fact that the conformal tower for bound-states is essentially a short-distance phenomenon produced by the singular behaviour of the potential at the centre.

#### IV. DISCUSSION AND COMPARISON WITH EXPERIMENT

In this section we will assume that QED<sub>3</sub> theory is in the strong-coupling regime characterized in Sec. III C and investigate the consequences of this assumption for the spin response observed in neutron scattering measurements.

The dispersion of the exciton mode can be read off from Eq. (23) and Eq. (24) to be

$$\omega_{\text{res}}(\mathbf{p}) = \sqrt{\omega_{\text{sg}}^2(\mathbf{p}) - p_c^2}, \quad (28)$$

where  $\omega_{\text{sg}}(\mathbf{p})$  is the “spin gap,” given by the minimum of the particle-hole continuum. With the linear Dirac spectrum for spinons, it is

$$\omega_{\text{sg}}(\mathbf{p}) = v_F^2 p_x^2 + v_\Delta^2 p_y^2,$$

where we have now restored the Fermi and gap velocities. In this formula,  $p_x||v_F$  is the component of the wave vector measured from the given node in the nodal direction and  $p_y||v_\Delta$  is the one in the perpendicular direction. There is one dispersion branch for each node. Due to the strong anisotropy  $v_\Delta/v_F \ll 1$ , the spin gap is much more sensitive to the changes of  $\mathbf{p}$  in the nodal direction. This causes the dispersion (28) to assume a characteristic shape shown in FIG. 3. This is in qualitative agreement with experiment if we identify the exciton mode with the observed resonance peak [8]. We will now discuss some features of the dispersion.

In the diagonal direction, FIG. 3(a), there are three exciton branches. Each of the nodes on the same diagonal line contribute one branch, and the other two nodes produce overlapping branches. They all cross at  $(\pi, \pi)$  and hence a strong resonance is expected here. The overlapping branch is rather flat. Its curvature is determined by the ratio  $v_\Delta/v_F$ . It quickly enters the continuum away from  $(\pi, \pi)$  and is, then, presumably damped. The other two branches fall off rather steeply (due to the square root in  $\omega_{\text{res}}$ ) and terminate a distance  $p_c/v_F$  away from the corresponding nodes.

In the parallel direction, FIG. 3(b), there are only two sets of overlapping branches, each from a pair of nodes that map to each other upon reflection about the parallel line. Here, too, we observe a crossing at  $(\pi, \pi)$  and, therefore, an enhanced response. The absence of the flat branch means that the momentum width of the resonance at  $(\pi, \pi)$  is only bound by the momentum resolution of the experiment in this direction. Again, the modes disperse down to zero energy at an incommensurate position  $(\pi \pm \delta_{\text{inc}}, \pi)$  where

$$\delta_{\text{inc}} = \frac{2(\pi - 2k_F) - \sqrt{2}p_c/v_F}{1 + v_\Delta^2/v_F^2} \lesssim 2(\pi - 2k_F) - \sqrt{2}p_c/v_F, \quad (29)$$

and the approximation is made for  $v_\Delta/v_F \ll 1$ .

In our Schrödinger equation approximation, the strength of the peak is given by  $|\psi_n(0, p_c)|^2$  at the resonance ( $p_M = p_c$ ) and is the same for different momenta. That is, the whole branch below the continuum spin gap has the same intensity. This does not agree with experiments in which the resonance peak appears to go away for low energies.

We also briefly note the effects of doping,  $x$ , on the dispersion of the exciton. In our formulation, doping enters through the dependence of the gauge-field mass,  $m(x)$ , the position of the nodes,  $k_F(x)$ , and the spin gap,  $\omega_{\text{sg}}(\mathbf{p}, x)$ . The gauge-field mass scales with  $T_c$  [17, 21]. Thus, it decreases with underdoping and vanishes at the underdoped superconducting transition. As we approach half-filling, the nodal points move towards  $(\pi/2, \pi/2)$  and  $k_F$  increases upon underdoping. This causes the spin gap to decrease [35]. From our scaling relations in Sec. III C, we see that the value of  $p_c(x) \sim m(x)$  also decreases with underdoping. Based on these trends, we can expect that with underdoping, and hence with decreasing  $T_c$ :

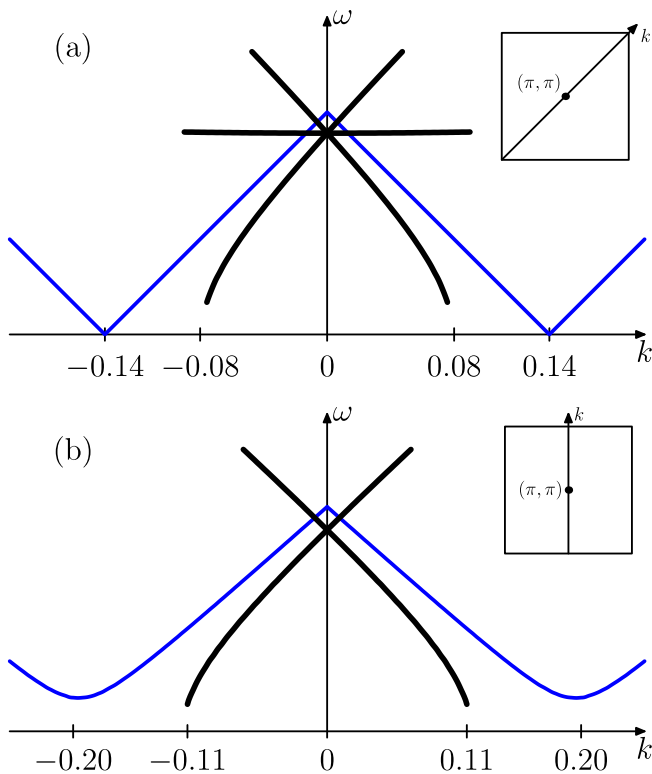


FIG. 3: (color online) The dispersion branches of the exciton in (a) the diagonal direction; and (b) the parallel direction, as shown in the insets. The wave vectors are in reciprocal lattice units, and the origin is at  $(\pi, \pi)$ . The value of parameters used are  $v_{\Delta}/v_F = 0.15$ ,  $k_F = 0.4\pi$  and  $p_c/v_F = \pi/16$ . The continuum spin gap is shown by the thick blue line and vanishes at the nodes.

(i) the resonance energy  $\omega_{\text{res}}$  decreases and merges with the decreasing spin gap; and (ii) the incommensurability  $\delta_{\text{inc}}$  decreases and merges with the nodal points. These are in qualitative agreement with experiment [8, 36–38]. We note, in contrast, that if  $k_F$  remains fixed while  $T_c$  changes in a set of experiments, Eq. (29) predicts that the incommensurability  $\delta_{\text{inc}}$  will *increase* linearly with decreasing  $T_c$ . Underdoping, however, increases  $k_F$ , hence the available area for the incommensurate structure shrinks.

The resonance and the incommensurate features go away at the transition, where  $m = T_c = 0$ . As  $T_c \rightarrow 0$  the resonance merges in with the continuum response. In our theory, we interpret the absence of a resonance in La-based cuprates with an anomalously small  $T_c$  compared to other cuprate families, as the difficulty to discern such a merging feature. If this is indeed what is happening, the same behavior should be seen in other families as  $T_c \rightarrow 0$ . Of course, it is possible that the absence of the resonance in La-cuprates is due to the different physics, that would give rise to stripes, for example.

## V. CONCLUSION

We have studied the problem of particle-hole bound states of spinons (excitons) in the QED<sub>3</sub> effective theory of a phase-fluctuating  $d$ -wave superconductor. This theory contains a massive gauge-field with an exact conformal propagator at high-energies. We employed a ladder approximation and derived an approximate Schrödinger-like equation for the bound states. We discussed the conditions for the existence of excitons and concluded that they would exist in the strong-coupling regime. We deduced the dispersion of the excitons and compared our results with neutron scattering measurements in cuprates.

This work complements the earlier work of Herbut and Lee [21], who discuss the continuum spin response in QED<sub>3</sub> in a low-energy approximation. It was found there that dispersing incommensurate and commensurate peaks similar to the resonance structure exist in the continuum. The qualitative behaviour of this continuum spectrum remains the same when higher-energy effects are included, but the numerical values of spin gap are reduced and are in fact close to the experimentally-observed range of resonance energies [35]. Thus, the continuum spectrum must be accounted for in extracting information on the exciton spectrum from experiments with a finite energy and momentum resolution.

Our vertex function is by definition gauge-dependent. In this work we used a non-local gauge-fixing term,  $\xi D(p)\hat{p}_\mu\hat{p}_\nu$ , in the gauge-field propagator with a momentum-independent parameter  $\xi$ . However, this is not enough to ensure the gauge invariance of the response for  $D(p)$  given by Eq. (2): enforcing the Ward-Takahashi identity for the bare spinon propagator yields [27] a momentum-dependent parameter  $2/3 < \xi(p) < 1$ , with the lower and higher bounds corresponding to the ultraviolet and infrared limits, respectively. A renormalization-group analysis on the original dual theory of Ref. 15, from which one can derive the action in Eq. (1), has been performed in Ref. 24. It was found that the charge  $g$  cannot be renormalized due to the non-analyticity of the spinon polarization  $\sim |p|$ . So, within our ladder approximation and for the bare value  $g = 1$ , it is likely that the gauge-invariant response is not in the strong-coupling regime. Further study of the gauge-invariant response seems necessary.

More comprehensive numerical studies of this problem will be very useful. They can be applied, at various stages, to the original vertex equations, or to the Schrödinger equation for the bound states. Finally, it is interesting to see whether other spin-collective modes, say triplets, can be formed in QED<sub>3</sub>.

## Acknowledgment

This research was supported by the NSERC of Canada and the CIAR. B.H.S. would like to thank M. Case, M. Franz, A. Furusaki, K. Kaveh, and N. Nagaosa for valu-

able discussions, and I.F.H. to D. Lee for a collaboration in the early stages of this project.

Then, keeping in mind that  $L = r \times p$ , from Eq. (17) we find

## APPENDIX A: DERIVATION OF EQ. (18)

We decompose the generalized response into symmetric and anti-symmetric components as  $\Phi' = \mathbb{1}\phi' + i\sigma \cdot \phi'_A$ .

$$\left[ \frac{p^2}{4} - \partial \cdot \partial - \lambda \cosh^2 |L/2| D(r) \right] \phi'(r, p) + i \frac{\lambda}{2} \sinh |L| D(r) \hat{L} \cdot \phi'_A(r, p) = \delta^{(3)}(r), \quad (\text{A1})$$

$$\left[ \frac{p^2}{4} - \partial \cdot \partial + \lambda \sinh^2 |L/2| D(r) \hat{L} \hat{L} \right] \phi'_A(r, p) + i \frac{\lambda}{2} \sinh |L| D(r) \hat{L} \phi'(r, p) = 0. \quad (\text{A2})$$

These are a set of coupled Schrödinger equations. However, we notice that the second equation contains a *repulsive* potential and consequently has presumably no negative-energy bound-states. Thus, for  $|p| > 0$ , its Green's function drops exponentially with increasing distance. In order to account for its effects on the bound states of the first equation, we may then solve the second equation for finite  $p$  simply as

$$\phi'_A(r, p) \approx -i \frac{2\lambda}{p^2} \sinh |L| D(r) \hat{L} \phi'(r, p).$$

By plugging this expression into the first equation we have  $[(p/2)^2 - \partial \cdot \partial - V_{\text{eff}}(r)]\phi'(r, p) = \delta^{(3)}(r)$ , where

$$V_{\text{eff}}(r) = \lambda \left[ 1 - \frac{4\lambda}{p^2} \sinh^2 |L/2| D(r) \right] \cosh^2 |L/2| D(r).$$

For  $0 < |p| < 2m$ , due to the exponential fall-off of  $D(r)$  (see Appendix B), we have

$$\frac{4}{p^2} \sinh^2 |L/2| D^2(r) \approx \frac{|r \times p|^2}{16r^2 p^2} D(r).$$

Thus, we obtain Eq. (18). For  $|p| > 2m$  we still find the same behaviour as above at short distances. But, for large distance, the  $\sim \lambda^2$  term overwhelms the other term and we have

$$V_{\text{eff}}(r \gg \frac{1}{|p| - 2m}) \sim -\frac{\lambda^2}{p^2} \sinh^2 |L| D^2(r),$$

as claimed in Eq. (20)

## APPENDIX B: REAL-SPACE GAUGE-FIELD PROPAGATOR

Here we derive the real-space interaction  $D(r)$ . Since there is a gap in the low energy limit, we expect an exponential decay in the long-distance behaviour of  $D(r)$ .

Also, the  $1/|p|$  tail in the high-energy limit should translate to a  $1/r^2$  singularity at short distances. We start by noting that

$$D(r) = \frac{m}{4\pi r} \int_0^{\Lambda/2m} F(1/2z) \sin(2m|r|z) dz \quad (\text{B1})$$

$$\equiv \tilde{D}(r) - \frac{m}{8|r|}, \quad (\text{B2})$$

where  $\Lambda$  is an ultraviolet cutoff and

$$\tilde{D}(r) = \frac{m}{8\pi|r|} \int_{-\Lambda/2m}^{+\Lambda/2m} \frac{1+z^2}{z^2} \tan^{-1} z \sin(2m|r|z) dz. \quad (\text{B3})$$

We compute  $\tilde{D}(r)$  using contour integration. To this end, we need to choose two branch-cuts to define  $\tan^{-1} z$ . We take them to be  $[+i, +i\infty)$  and  $[-i, -i\infty)$  such that  $z - i = r_1 e^{i\theta_1}$  with  $-\frac{3\pi}{2} < \theta_1 < \frac{\pi}{2}$  and  $z + i = r_2 e^{i\theta_2}$  with  $-\frac{\pi}{2} < \theta_2 < \frac{3\pi}{2}$ . Then,

$$\tan^{-1} z = -\frac{i\pi}{2} + \log \frac{r_2}{r_1} + i(\theta_2 - \theta_1).$$

We take a contour  $C$  that includes the real axis and closes on itself in the upper-half plane, except that it avoids the upper branch-cut by tracing the path  $C_1 = -F(0^+) \cup F(0^-)$  where  $F(\varepsilon) = [\varepsilon + i, \varepsilon + i\infty)$ . So, we can now write

$$\begin{aligned} \tilde{D}(r) &= \frac{m}{8\pi r} \Im \left[ \left( \oint_C - \int_{C_1} \right) \frac{1+z^2}{z^2} \tan^{-1} z e^{2im|r|z} dz \right] \\ &= \frac{m}{8r} \left[ 1 + \int_1^\infty \frac{u^2 - 1}{u^2} e^{-2m|r|u} du \right]. \end{aligned} \quad (\text{B4})$$

So, we find

$$D(r) = \frac{m}{8r} \int_1^\infty \frac{u^2 - 1}{u^2} e^{-2m|r|u} du \quad (\text{B5})$$

$$= \frac{e^{-2m|r|}}{16r^2} - \frac{m}{8|r|} E_2(2m|r|). \quad (\text{B6})$$

Note that  $D(r) > 0$ . Here,  $E_n(x) = \int_1^\infty e^{-ux} du/u^n$  is the exponential integral. For  $n = 2$  it has the following asymptotic behaviour

$$E_2(x) = \begin{cases} e^{-x} \left( \frac{1}{x} - \frac{2}{x^2} + \dots \right), & x \rightarrow \infty, \\ 1 + (\gamma_E - 1)x + \dots, & x \rightarrow 0, \end{cases}$$

where  $\gamma_E$  is the Euler-Mascheroni constant. It leads in

turn to the following asymptotic behaviour for  $D(r)$ :

$$D(r \rightarrow \infty) = \frac{e^{-2m|r|}}{64m|r|^3} + O(|r|^{-4}e^{-2m|r|}), \quad (\text{B7})$$

$$D(r \rightarrow 0) = \frac{1}{16r^2} - \frac{m}{4|r|} + O(m^2 \log(m|r|)). \quad (\text{B8})$$

- 
- [1] H. F. Fong *et al.*, Nature **398**, 588 (1999).
  - [2] H. He *et al.*, Physical Review Letters **86**, 1610 (2001).
  - [3] H. F. Fong *et al.*, Physical Review Letters **75**, 316 (1995).
  - [4] S. M. Hayden, H. A. Mook, P. Dai, T. G. Perring, and F. Doğan, Nature **429**, 531 (2004).
  - [5] V. Hinkov *et al.*, cond-mat/0601048.
  - [6] K. Yamada *et al.*, Physical Review Letters **75**, 1626 (1995).
  - [7] K. Yamada *et al.*, Physical Review B **57**, 6165 (1998).
  - [8] N. B. Christensen *et al.*, Physical Review Letters **93**, 147002 (2004).
  - [9] J. M. Tranquada *et al.*, Nature **429**, 534 (2004).
  - [10] H. He *et al.*, Science **295**, 1045 (2002).
  - [11] P. Bourges *et al.*, Physica C: Superconductivity **424**, 45 (2005).
  - [12] V. Hinkov *et al.*, Nature **430**, 650 (2004).
  - [13] M. Franz and Z. Tešanović, Physical Review Letters **87**, 257003 (2001).
  - [14] I. F. Herbut, Physical Review Letters **88**, 047006 (2002).
  - [15] I. F. Herbut, Physical Review B **66**, 094504 (2002).
  - [16] M. Franz, Z. Tešanović, and O. Vafeck, Physical Review B **66**, 054535 (2002).
  - [17] I. F. Herbut, Physical Review Letters **94**, 237001 (2005).
  - [18] T. Appelquist, D. Nash, and L. C. R. Wijewardhana, Physical Review Letters **60**, 2575 (1988).
  - [19] P. Maris, Physical Review D **54**, 4049 (1996).
  - [20] B. H. Seradjeh and I. F. Herbut, Physical Review B **66**, 184507 (2002).
  - [21] I. F. Herbut and D. J. Lee, Physical Review B **68**, 104518 (2003).
  - [22] We have corrected for a factor of two in the gauge-field propagator compared to Ref. 21 due to the presence of two bosonic order parameters in the original theory of Refs. 15 and 17.
  - [23] I. F. Herbut and Z. Tešanović, Physical Review Letters **76**, 4588 (1996); *ibid* **78**, 980 (1997).
  - [24] D. J. Lee and I. F. Herbut, Physical Review B **67**, 174512 (2003).
  - [25] C. J. Burden, Nuclear Physics B **387**, 419 (1992).
  - [26] V. P. Gusynin and M. Reenders, Physical Review D **57**, 6356 (1998).
  - [27] V. Gusynin, A. Hams, and M. Reenders, Physical Review D **63**, 045025 (2001).
  - [28] D. Nash, Physical Review Letters **62**, 3024 (1989).
  - [29] G. D. Mahan, Physical Review Letters **18**, 448 (1967).
  - [30] G. D. Mahan, Physical Review **153**, 882 (1967).
  - [31] W. E. Caswell and G. P. Lepage, Physical Review A **18**, 810 (1978).
  - [32] T. W. Allen and C. J. Burden, Physical Review D **53**, 5842 (1996).
  - [33] L. D. Landau and E. M. Lifshitz, *Quantum Mechanics: Non-Relativistic Theory*, 3rd ed. (Butterworth-Heinemann, Burlington, MA, 2003) §35.
  - [34] H. E. Camblong, L. N. Epele, H. Fanchiotti, and C. A. García Canal, Physical Review Letters **85**, 1590 (2000).
  - [35] B. H. Seradjeh, PhD thesis, Simon Fraser University, 2006.
  - [36] H. F. Fong *et al.*, Physical Review B **61**, 14773 (2000).
  - [37] P. Dai, H. A. Mook, R. D. Hunt, and F. Doğan, Physical Review B **63**, 054525 (2001).
  - [38] S. Pailhès *et al.*, Physical Review Letters **96**, 257001 (2006).